Interaction Mechanism between Cellobiose and Imidazolium Halide-based Ionic Liquids

Ling Yang, Hong Peng,* Hongwei He, Ling Liu, Guiming Fu, Yuhuan Liu, and Yin Wan

Ionic liquids (ILs) are excellent solvents for cellulose, but the dissolution mechanism is not deeply understood. In the present study, cellobiose was used as a model of cellulose, and the imidazolium halide-based ILs with the same cation of 1-butyl-3-methylimidazolium ($Bmim^+$) including BmimCl, BmimBr, and BmimI were used as solvents. The interaction mechanism between the ILs and cellobiose was analyzed by carbon-13 nuclear magnetic resonance (^{13}C NMR). The results showed that the strength of hydrogen bonds formed between the hydroxyl groups of cellobiose and the ILs was greatly affected by the position of hydroxyl groups and the electro-negativity and size of the anions. Compared with the secondary alcoholic hydroxyl groups, the primary alcoholic hydroxyl groups (C6–OH and C12–OH) on the glucopyranose rings of cellobiose more easily formed hydrogen bonds with the ILs. The strength of hydrogen bonds formed between the protons on the imidazolium cation and cellobiose varied with the positions of the protons. The formation of hydrogen bonds between the halogen anions and cellobiose was the main reason for the dissolution of cellobiose in the ILs. The ability of the three ILs to form hydrogen bonds with cellobiose followed the order: BmimCl > BmimBr > BmimI.

DOI: 10.15376/biores.18.1.1590-1601

Keywords: Cellobiose; Ionic liquids; Hydrogen bond; Cellulose; ^{13}C NMR analysis; Chemical shift

Contact information: Engineering Research Center of Biomass Conversion, Ministry of Education, Nanchang University, Nanchang, Jiangxi 330047, P R. China;
** Corresponding author: penghong@ncu.edu.cn*

INTRODUCTION

Cellulose is the most abundant natural polymer material and renewable biomass resource in nature. Its good biocompatibility, biodegradability, and renewable advantages make cellulose one of the potential green raw materials in the fields of energy, chemical industry, and polymer materials (Pinkert *et al.* 2009; Seddiqi *et al.* 2021). Cellulose is a linear polymer composed of D-glucopyranose linked by *β*-1,4-glycosidic bonds (O'Sullivan 1997; Klemm *et al.* 2005). The basic unit of cellulose is cellobiose, and the two glucose units are rotated by 180° in the plane, leading to the directionality of the cellulose molecule (Xiong *et al.* 2014). The inverted structure of adjacent glucose units enables the cellulose chain to unfold in a straight line, resulting in strong rigidity and crystallinity of natural cellulose (Valert 2010). This special structure of cellulose makes it difficult to dissolve in water and conventional solvents, and this greatly limits the application of cellulose (Sansaniwal *et al.* 2017). Therefore, the development of solvents that can effectively dissolve cellulose and destroy the crystalline structure of cellulose can be expected to play a pivotal role in expanding the industrial application of cellulose.

Ionic liquids (ILs) composed of organic cations and organic or inorganic anions are

a new class of green solvents (Hunt *et al.* 2015; Sanchez *et al.* 2020). The ILs are mostly liquid at room temperature and they have many advantages such as thermal stability, low melting point, designability, and recyclability. They have shown potential applications in material modification, reaction medium, and component separation (Singh and Savoy 2020). Some ILs show strong ability to dissolve cellulose and destroy the crystalline structure of cellulose during the pretreatment process of lignocellulosic biomass, which can significantly improve the subsequent conversion efficiency of the raw materials (Usmani *et al.* 2020). However, up to now, no systematic conclusion has been obtained on the dissolution mechanism of ILs with different chemical structure to dissolve cellulose. Therefore, the theoretical support for the scientific design of ILs that can efficiently pretreat lignocellulose is insufficient. Some researchers have found that the ability of ILs to dissolve cellulose is closely related to the formation of hydrogen bonds between ILs and cellulose (Sanchez-Badillo *et al.* 2021). These ILs can break the hydrogen bond network in cellulose and form new ones with cellulose, leading to the final dissolution of cellulose (Krishna and Jiang 2015). Li *et al.* (2015) found that the anions of ILs are usually small in size, and they can insert themselves into the cellulose chain to destroy the intramolecular hydrogen bond network of natural cellulose and form new hydrogen bonds. This appears to be a key factor for cellulose dissolving in ILs. Xu *et al.* (2015) found that the solubility of cellulose increases with the increase of the alkyl side chain within a certain range when the C2 position on the imidazole ring of the imidazolium ionic liquid is not substituted. The extension of the alkyl side chain increases its electron-donating ability, which leads to an increase in the acidity of hydrogen atoms including C2–H and C4–H, and promotes the formation of hydrogen bonds between the cation and the hydroxyl oxygen of cellulose (Xu *et al.* 2015). However, when the alkyl side chain of imidazolium cation is further extended, the steric hindrance effect is strengthened and the hydrophilicity is weakened, resulting in a decrease in the solubility of cellulose (Xu *et al.* 2015). In general, the dissolution of cellulose in ILs is greatly related to the formation of hydrogen bonds between the ILs and cellulose. Therefore, it is of great significance to study the formation law of hydrogen-bonding between ILs and cellulose. The deep understanding of the dissolution mechanism of cellulose in ILs is helpful for designing efficient ILs to realize the dissolution, separation, and utilization of cellulose.

In the present study, cellobiose was used as the model of cellulose, and the imidazolium halide-based ILs 1-butyl-3-methylimidazolium chloride (BmimCl), 1-butyl-3-methylimidazolium bromide (BmimBr), and 1-butyl-3-methylimidazolium iodide (BmimI) were used as solvents. The dissolution mechanism of cellobiose in these imidazolium halide-based ILs were obtained based on ^{13}C-nuclear magnetic resonance (^{13}C NMR) analysis. 1-Butyl-3-methylimidazolium fluorine (BmimF) is known to be highly corrosive; therefore, it was not considered in the present study.

EXPERIMENTAL

Materials

Cellobiose (> 99%) was purchased from Shanghai Lanji Technology Development Co., Ltd., China. BmimCl (> 99%), BmimBr (> 99%), and BmimI (> 99%) were purchased from Shanghai Chengjie Chem. Co., Ltd., China. The chemical structures of cellobiose and ILs are shown in Fig. 1. The ILs were dried in a vacuum oven for 24 h at 150 °C before use. Water content in each ionic liquid measured using Karl–Fischer method was less than

1000 ppm. Deuterated dimethyl sulfoxide (DMSO-d_6) (> 99.9%) which was used as solvent for nuclear magnetic resonance (NMR)-analysis, was purchased from Shanghai Macklin Biochemical Technology Co., Ltd., China.

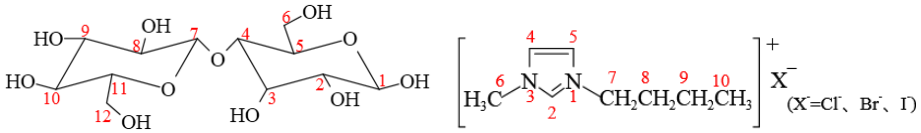

Fig. 1. Schematic structure and numbering of C in cellobiose, BmimCl, BmimBr, and BmimI

Methods

To elucidate the interaction between cellobiose and the ILs, the changes in ^{13}C chemical shifts of the cellobiose and the ILs were obtained through ^{13}C NMR technique. The ^{13}C NMR spectra were recorded on a Bruker Avance 600 MHz spectrometer (Bruker, Karlsruhe, Germany) with a 5 mm PABBO probe at 25 °C. The ^{13}C NMR spectra were obtained at 100.6 MHz after 1024 scans. Before analysis, cellobiose (20 to 100 mg) was added to a NMR tube with 0.5 mL of DMSO-d_6 and 200 mg of IL, resulting in mass concentration of cellobiose ranging from 10 wt% to 50 wt% (cellobiose/IL, mg/mg). As a control, 20 mg of the cellobiose and 200 mg of the pure ILs were separately dissolved in 0.5 mL of DMSO-d_6. The relative changes in the chemical shifts were calculated according to Eqs. 1 and 2:

$$\Delta\delta_{IL} = \delta_{IL\ in\ mixture} - \delta_{Pure\ IL} \quad (1)$$

$$\Delta\delta_{Cellobiose} = \delta_{Cellobiose\ in\ mixture} - \delta_{Pure\ cellobiose} \quad (2)$$

RESULTS AND DISCUSSION

^{13}C NMR Analysis of Cellobiose and ILs

The ^{13}C NMR spectra of cellobiose, the representative ionic liquid BmimCl, and the solution obtained by dissolving 30 wt% cellobiose in BmimCl (BmimCl + 30 wt% BmimCl) are shown in Fig. 2. The identification of peaks referred to the data shown in the literature (Xu *et al.* 2010; Amarasekara *et al.* 2011; Xu *et al.* 2014). In order to facilitate differentiation, the carbon atoms of the ILs were assigned as IC, and those of cellobiose were labelled as C. For cellobiose (Fig. 2a), the peaks at δ 102.59, 96.08, 80.18, 76.20, 75.89, 74.48, 74.15, 73.91, 72.73, 69.46, 60.45, and 59.97 ppm were assigned to C7, C1, C4, C11, C9, C5, C3, C2, C8, C10, C12, and C6, respectively. It can be clearly found that even though the carbon positions on the two glucose units of cellobiose were the same, there were certain differences in chemical shifts, such as those between C6 and C12, between C2 and C8, and between C3 and C9. The results showed that the distribution of electron cloud on the two glucose units of cellobiose was not exactly the same, leading to the difference in the chemical shift at the same position on the glucose unit at the reducing end and the non-reducing end.

The typical ^{13}C NMR spectrum of BmimCl is shown in Fig. 2b, and the carbon chemical shifts of the three ILs including BmimCl, BmimBr, and BmimI are summarized in Table 1. Because these three ILs had the same cation, the chemical shifts of the carbons at the same position were similar. However, because of the difference in electro-negativity

of the anions, the chemical shifts of these carbon atoms varied slightly. The order of chemical shifts of IC2, IC4, and IC5 on the imidazole ring was almost the same as that of electro-negativity strength of halide anions (Cl^- > Br^- > I^-). It was suggested that as the electro-negativity of the halide anion strengthened, the hydrogen bond strength between the halide anion and the protons at IC2, IC4, and IC5 (IC2–H, IC4–H, and IC5–H) on the imidazole ring increased, resulting in the decrease of electron cloud density around IC2, IC4, and IC5, and the increase of their chemical shifts (Xu and Zhang 2015). The chemical shifts of IC2 differed greatly among BmimCl, BmimBr, and BmimI, indicating that the strength of hydrogen bonds formed between IC2–H and the halogen anions was remarkably affected by the electro-negativity of the anions. The chemical shift differences of IC4 and IC5 among the three ILs were smaller than that of IC2, indicating that the acidity of IC4–H and IC5–H was weaker than that of IC2–H. At the same time, the order of the chemical shifts of IC6 and IC7 on the alkyl side chain, which directly linked to the N atom on the imidazole ring, was BmimCl < BmimBr < BmimI, which was opposite to that of the electro-negativity of the halogen anion. A possible reason was that the stronger electro-negativity of the halogen anion resulted in the higher electron cloud density around the IC6 and IC7 atoms and the movement of chemical shift to the high field (Xu and Zhang 2015). The above results showed that the acidity of protons at different positions on 1-butyl-3-methylimidazolium varied much.

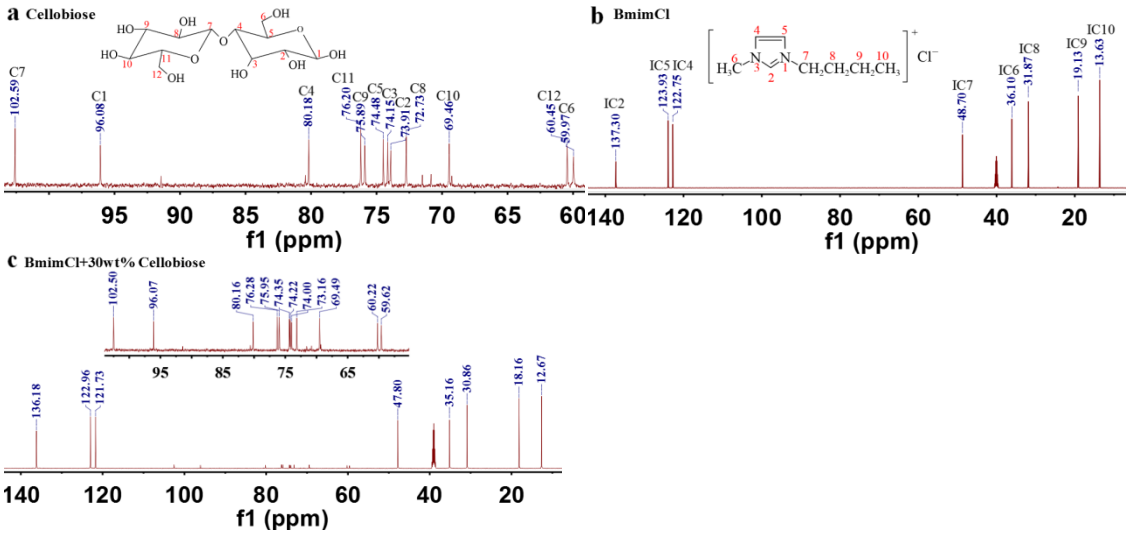

Fig. 2. ^{13}C NMR spectra of (a) cellobiose; (b) BmimCl; and (c) BmimCl + 30 wt% cellobiose (25 °C, in DMSO-d_6)

Table 1. Chemical Shifts of Carbons of BmimCl, BmimBr, and BmimI (25 °C, in DMSO-d_6)

ILs	Chemical Shift δ (ppm)							
	IC2	IC4	IC5	IC6	IC7	IC8	IC9	IC10
BmimCl	137.30	122.75	123.93	36.10	48.70	31.87	19.13	13.63
BmimBr	136.94	122.67	123.86	36.31	48.84	31.84	19.13	13.66
BmimI	136.82	122.63	123.87	36.62	49.01	31.77	19.16	13.73

Analysis of the Interaction between Cellobiose and ILs

DMSO-d_6 is an aprotic solvent with almost negligible dissociation into solvated ions. Thus, DMSO-d_6 had little effect on the formation of hydrogen bonds between the ILs and cellobiose, and its main role was to dissociate the ion pairs of ILs into solvated anions and cations (Xu and Zhang 2015). Therefore, the change in chemical shifts could be used to evaluate the strength of the interaction between the ILs and cellobiose. A representative ^{13}C NMR spectrum of the sample after dissolving 30 wt% cellobiose in BmimCl (BmimCl + 30 wt% cellobiose) is shown in Fig. 2c. The relative changes in chemical shifts of carbons at different position of cellobiose after dissolving in BmimCl, BmimBr, and BmimI are summarized in Figs. 3 and 4. The cellobiose concentration varied from 10 wt% to 50 wt%.

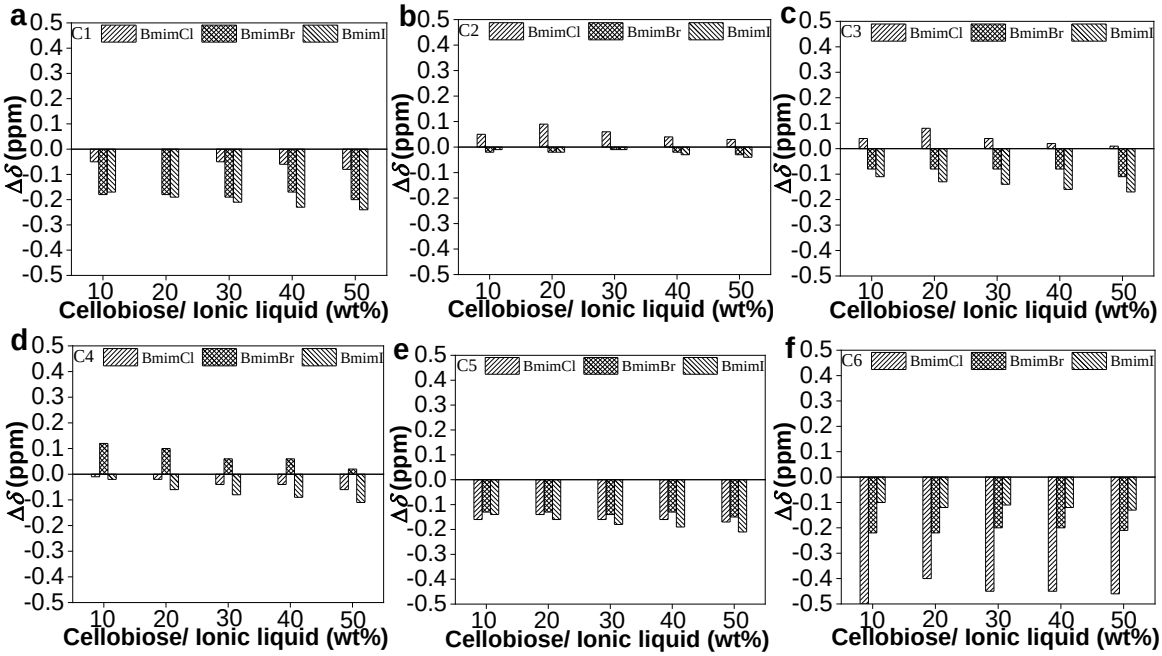

Fig. 3. Relative change in chemical shifts of carbons at the reducing end of cellobiose compared with the pure cellobiose (in DMSO-d_6)

Cellobiose consists of two glucopyranose units. One is the reducing end and the other is the non-reducing end. There are four free alcoholic hydroxyl groups at the reducing end and non-reducing ends. Among those hydroxyl groups, the C6–OH and C12–OH are primary alcoholic hydroxyl groups, and the rest are secondary alcoholic hydroxyl groups (Fig. 1). Theoretically, these hydroxy protons can form hydrogen bonds with proton acceptors, and the hydroxy oxygens can form hydrogen bonds with protons. As shown in Figs. 3a and 3c, and 4c, the relative chemical shift changes ($\Delta\delta$) of C1, C3, and C9 after cellobiose with different concentration dissolved in the ILs were in the order: BmimI < BmimBr < BmimCl. The relative chemical shift changes of C1, C3, and C9 were almost negligible ($|\Delta\delta| < 0.05$ppm) when cellobiose was dissolved in BmimCl, indicating that BmimCl hardly formed hydrogen bonds with C1–OH, C3–OH, and C9–OH, or the hydrogen bonds formed were extremely weak. At the same time, the chemical shifts of C1, C3, and C9 moved to the high field after cellobiose was dissolved in BmimBr and BmimI, indicating that the electron cloud density around the C1, C3, and C9 atoms increased (Xu and Zhang 2015). A possible reason was that Br^- and I^- from BmimBr and BmimI formed hydrogen bonds with the protons of C1–OH, C3–OH, and C9–OH, respectively. The

relative chemical shift changes of C8 at the non-reducing end of cellobiose after it dissolved in ILs were in the order of BmimI < BmimBr < BmimCl (Fig. 4b). In addition, the chemical shift of C8 in BmimI solution nearly unchanged ($|\Delta\delta| < 0.05$ ppm), and the Δδ values of C8 in BmimBr and BmimCl were higher than 0 (Fig. 4b). The possible reason was that the acidic protons on the imidazolium cations of BmimBr and BmimCl, such as IC2–H, formed a hydrogen bond with the hydroxyl oxygen at the C8 position of cellobiose, resulting in the decrease of the electron cloud density around the C8 atom and the movement of chemical shift to the lower field (Zhang *et al.* 2010). Meanwhile, the acidity of the protons on the imidazolium cation of BmimI was too weak to form hydrogen bonds with C8–OH. The chemical shifts of C2 and C10 were almost unchanged ($|\Delta\delta| < 0.05$ ppm) (Figs. 3b and 4d), indicating that there was almost no hydrogen-bonding between C2–OH and C10–OH and the ILs. The chemical shift changes of C4, C5, C7, and C11 were caused by the redistribution of electron cloud on the glucopyranose rings (Figs. 3d and 3e, Figs. 4a and 4e) (Chen *et al.* 2011).

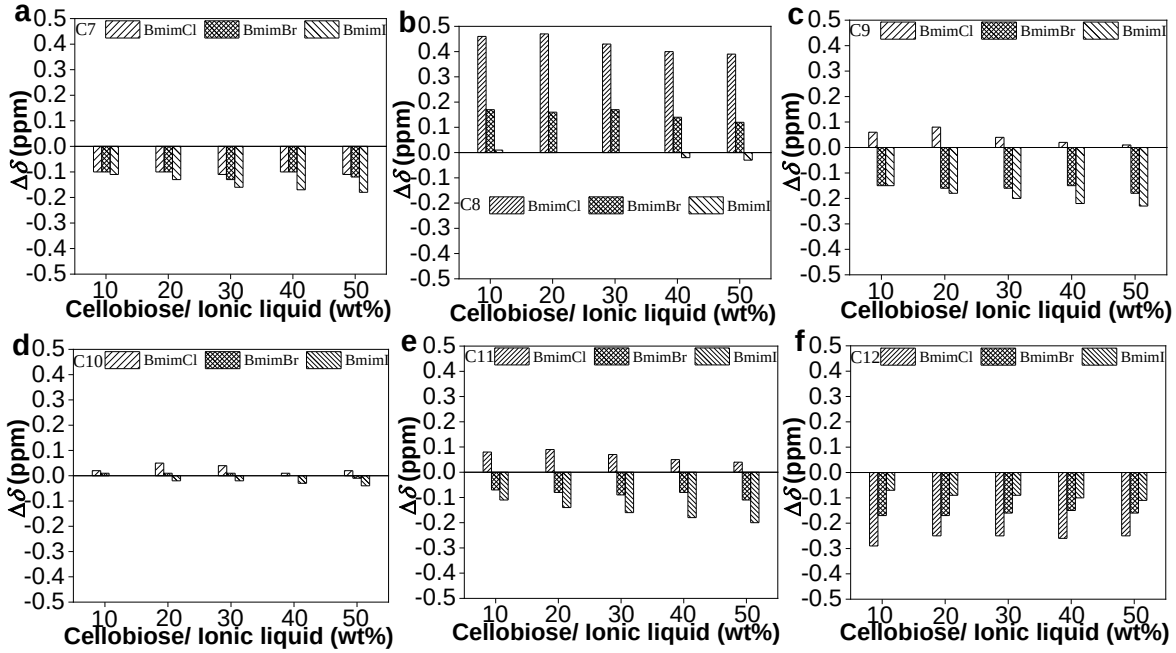

Fig. 4. Relative change in chemical shifts (in DMSO-d_6) of carbons at the non-reducing end of cellobiose compared with the pure cellobiose

The relative chemical shift changes of C6 and C12 (in DMSO-d_6) were in the order BmimCl < BmimBr < BmimI < 0 (Figs. 3f and 4f), indicating that the δ-values of C6 and C12 also shifted to the high field after the dissolution of cellobiose in the ILs (Xu and Zhang 2015). A possible reason was that the formation of hydrogen bonds took place between the halogen anions and the protons of C6–OH and C12–OH. Furthermore, according to the intensities of the relative chemical shift changes, the order of hydrogen bond strength between the anions and C6–OH and C12–OH was $Cl^- > Br^- > I^-$. The Kamlet-Taft (K-T) parameter β value is usually used to evaluate the hydrogen-bond accepting ability of ILs. Anions act as proton acceptor in the formation of hydrogen bonds, and their hydrogen-bond accepting ability is greatly affected by their structure. Usually, the anion with higher β value has stronger hydrogen-bond accepting ability (Zhang 2008). According to the experimental results obtained by Lungwitz and Spange (2008), the β

values of Cl^-, Br^-, and I^- are 0.94, 0.87, and 0.75, respectively, that is, the hydrogen-bond accepting ability is $Cl^- > Br^- > I^-$. In theory, the order of volume follows $Cl^- < Br^- < I^-$, and C6–OH and C12–OH are primary alcoholic hydroxyl groups with larger steric hindrance. Therefore, the anions with smaller size and stronger electro-negativity are more accessible to C6–OH and C12–OH and form strong hydrogen bonds, such as Cl^-. It can be seen from Figs. 3 and 4 that, compared with the secondary hydroxyl groups at the other positions, the primary hydroxyl groups at C6 and C12 were more likely to form hydrogen bonds with ILs, resulting in more obvious change in the chemical shifts of C6 and C12. This indicated that the formation of hydrogen bonds between C6–OH and C12–OH and ILs was possibly the main reason for the dissolution of cellobiose in the ILs. Finally, the intensity of the relative chemical shift change of C6 was greater than that of C12, implying that the strength of the hydrogen bond formed between C6–OH and the anions was stronger than that between C12–OH and the corresponding anions. In other words, the hydrogen bonds formed between the reducing end and the anion was stronger than that between the non-reducing end and the anion.

The relative changes in the chemical shifts of carbons at different positions of BmimCl, BmimBr, and BmimI are shown in Fig. 5. It can be clearly seen from Fig. 5 that compared with the pure ILs, the chemical shifts of carbon atoms at different position of the three ILs moved towards the high field when cellobiose with different concentration was dissolved in them, resulting in the $\Delta\delta$ values lower than zero. The results demonstrated that the electron cloud density on the imidazolium cations of ILs increased because of the interaction with cellobiose. It is noted from Fig. 5a that the chemical shifts of IC2 on the imidazole ring decreased as the cellobiose concentration increased from 10 wt% to 50 wt%, indicating that the chemical shift of IC2 moved towards the high field. The possible reason was that with the increase of cellobiose concentration, more hydroxyl oxygen from cellobiose formed hydrogen bonds with the acidic proton IC2–H at IC2 position on the imidazole ring (Hu *et al.* 2020; Xia *et al*. 2020). Simultaneously, the hydrogen bonds between IC2–H and the halogen anions were destroyed, leading to the increase of electron cloud density around the IC2 atom (Xu and Zhang 2015). Finally, the chemical shift moved to the high field, and the $\Delta\delta$ values kept decreasing (Xu and Zhang 2015). The $\Delta\delta$ value of IC2 was linear negative correlation with the cellobiose concentration, implying that the strength of hydrogen bond formed between IC2–H and cellobiose had a linear positive correlation with the cellobiose concentration. At the same time, the slope in the linear equation between the relative chemical shift change of IC2 and the cellobiose concentration was -0.0047, -0.0019, and -0.0016 for BmimCl, BmimBr, and BmimI, respectively, indicating that the influence of cellobiose concentration on the chemical shift change of IC2 followed the order BmimCl > BmimBr > BmimI. In other words, the IC2–H of BmimCl exhibited the strongest acidity, and it was most likely to form hydrogen bonds with hydroxyl oxygen of cellobiose (Xu and Zhang 2015).

Because the difference among the $\Delta\delta$ values was within the range of 0.05 ppm, the change in chemical shifts of IC4 and IC5 connected to N on the imidazole ring and IC8, IC9, and IC10 on the side chain butyl could be ignored with the change of cellobiose concentration (Figs. 5b, 5c, 5f, 5g, and 5h). This may be due to the weak acidity of the protons connected to these carbons, making them be difficult to form hydrogen bonds with the hydroxyl oxygen of cellobiose, resulting in that the influence of cellobiose concentration on the density of electron cloud around these carbon atoms was almost negligible (Xu and Zhang 2015). The relative change in chemical shifts of IC6 and IC7 on the side chain, which were directly connected to N on the imidazole ring, increased with

the increase of cellobiose concentration, and they showed a good linear positive correlation with the concentration of cellobiose (Figs. 5d and 5e). This indicated that the strength of the hydrogen bonds formed between IC6–H and IC7–H and cellobiose was linearly negatively correlated with the concentration of cellobiose. In addition, with the increase of cellobiose concentration, the chemical shift changes of IC6 and IC7 of BmimCl were more remarkable than those of BmimBr and BmimI. This result further indicated that the hydrogen bonds formed between BmimCl and cellobiose were stronger than those between BmimBr and BmimI and cellobiose. It could be concluded from the results given in Figs. 3, 4, and 5 that the ability of BmimCl, BmimBr, and BmimI to form hydrogen bond with cellobiose was in the order BmimCl > BmimBr > BmimI, which was consistent with that of the solubility of cellulose in BmimCl, BmimBr, and BmimI (Zhao *et al.* 2013).

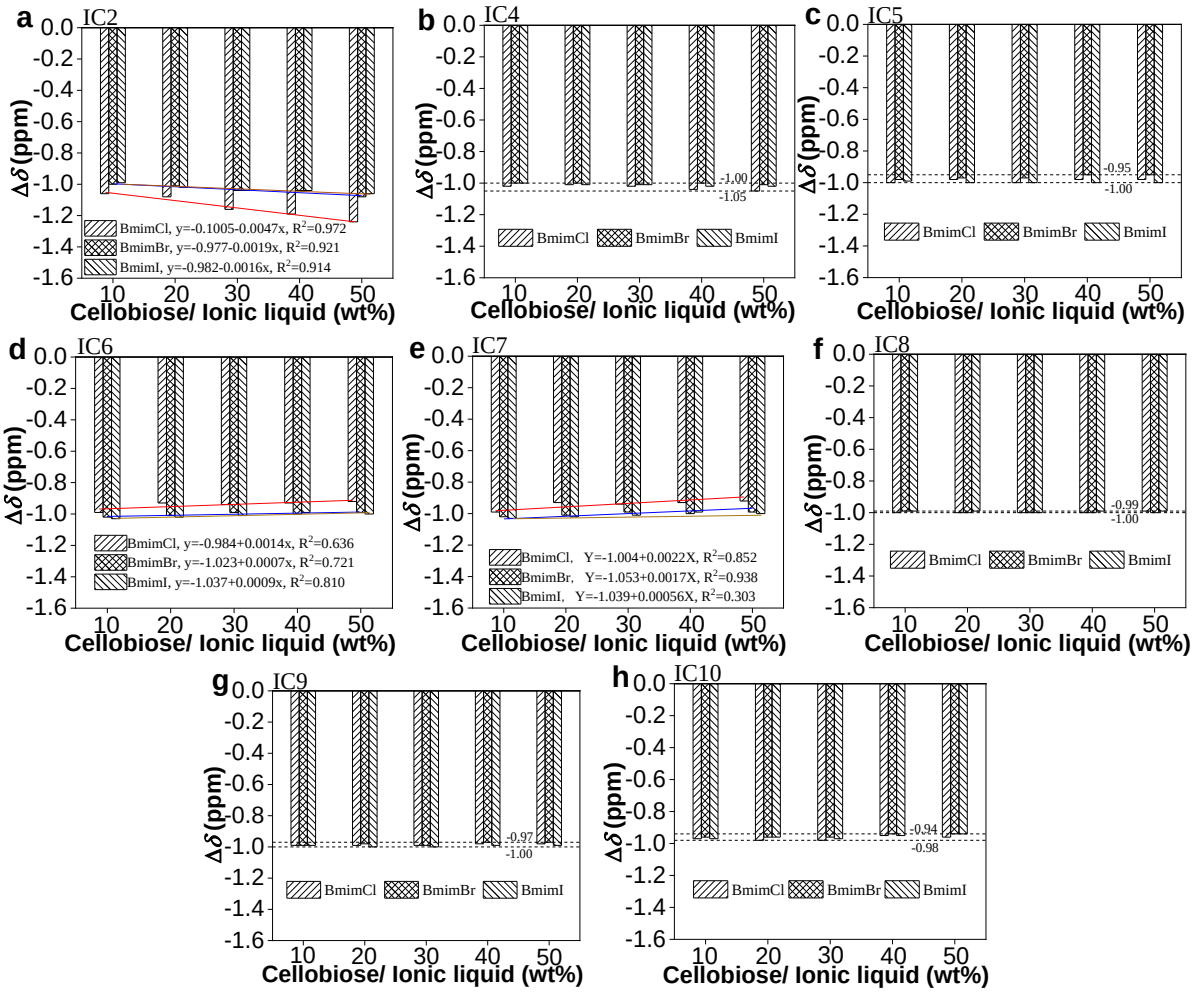

Fig. 5. Relative change in chemical shifts of the carbons (in DMSO-d_6) of ILs compared with the pure ILs

A possible interaction mechanism between cellobiose and the imidazolium halide-based ILs is shown in Fig. 6. According to the data shown in Figs. 3 and 4, the $\Delta\delta$ values of C1, C3, and C6 at the reducing end of cellobiose, and of C9 and C12 at the non-reducing end were lower than zero. It could be inferred that the density of electron cloud around C1, C3, C6, C9 and C12 increased possibly due to the anion. On the contrary, the $\Delta\delta$ values of C8 at the non-reducing end (Fig. 4) were higher than zero. It could be inferred that the

density of electron cloud around C8 decreased, possibly due to the cation. Therefore, it could be inferred that the anions of ILs mainly formed hydrogen bonds with the protons of C1–OH, C3–OH, and C6–OH at the reducing end of cellobiose, and of C9–OH and C12–OH at the non-reducing end. The acidic protons on the imidazolium cation mainly formed hydrogen bonds with the oxygen of C8–OH at the non-reducing end. The formation of hydrogen bonds between the ILs and the hydroxyl groups of cellobiose led to the destruction of intermolecular and intramolecular hydrogen-bonding network of cellobiose, thus promoting the dissolution of cellobiose in the ILs. At the same time, not all the hydroxyl groups of cellobiose could form strong hydrogen bonds with the ILs, such as C2–OH at the reducing end and C10–OH at the non-reducing end. Finally, the formation of hydrogen bonds between the anions and the hydroxyl groups of cellobiose was the key factor leading to the dissolution of cellobiose in the ILs. However, based on thermodynamics, cellulose molecule is much less translational free energy per glucose unit, leading to be much less soluble than cellobiose which is the model compound of cellulose. Thus, in the further, model compounds with higher molecular weight should be considered to evaluate the interaction between cellulose and ILs.

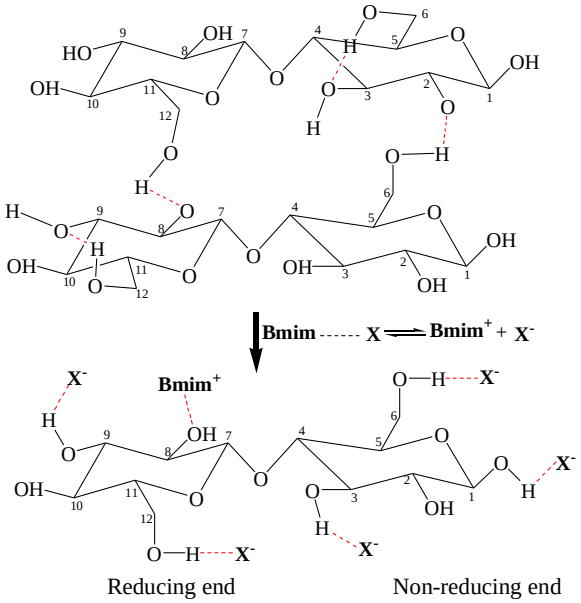

Fig. 6. Possible interaction mechanism of cellobiose with the imidazolium halide-based ILs

CONCLUSIONS

1. Three kinds of ionic liquids (ILs), each having the same cation of 1-butyl-3-methylimidazolium (BmimCl, BmimBr, and BmimI) were used to dissolve cellobiose, and the interaction mechanism was evaluated by using ^{13}C NMR.
2. The slight difference in the chemical shifts of carbons at the same position on the two glucose units of cellobiose suggested that the electron cloud distribution on the two glucose units was not completely the same. The acidity of protons on the imidazolium cation varied much among the three ILs.

3. The hydrogen bond strength between the hydroxyl groups of cellobiose and the ILs was clearly influenced by the position of hydroxyl groups and the electro-negativity and size of the anions. Compared with the secondary alcoholic hydroxyl groups, the ILs were more likely to form hydrogen bonds with the primary alcoholic hydroxyl groups (C6–OH and C12–OH) on the glucopyranosyl ring of cellobiose. The hydrogen bond formed between C6–OH at the reducing end and the anion was stronger than that formed between C12–OH at the non-reducing end and the anion.
4. The chemical shifts of carbons at different position on cellobiose were not remarkably affected by the concentration of cellobiose in the IL solution. The strength of the hydrogen bonds between cellobiose and IC2–H on the imidazolium cation was linearly positively correlated with the cellobiose concentration, while that between IC6–H and IC7–H and cellobiose was linearly negatively correlated with the concentration of cellobiose.
5. Both the anion and cation could form hydrogen bonds with cellobiose, but the formation of hydrogen bonds between the anion and cellobiose was the key factor for the dissolution of cellobiose in the ILs. The ability of the three ILs to form hydrogen bonds with cellobiose was in the order of BmimCl > BmimBr > BmimI.

ACKNOWLEDGMENTS

This work was financially supported by the National Natural Science Foundation of China (No. 22068025), and the Graduate Innovation Special Foundation Project of Jiangxi Province (No. YC2022-s099).

REFERENCES CITED

Amarasekara, A. S., Owereh, O. S., and Ezeh, B. (2011). "Interactions of D-cellobiose with *p*-toluenesulfonic acid in aqueous solution: A ^{13}C NMR study," *Carbohydr. Res.* 346(17), 2820-2822. DOI: 10.1016/j.carres.2011.09.032

Chen, Q. T., Xu, A. R., Li, Z. Y., Wang, J. J., and Zhang, S. J. (2011). "Influence of anionic structure on the dissolution of chitosan in 1-butyl-3-methylimidazolium-based ionic liquids," *Green Chem.* 13(12), 3446-3452. DOI: 10.1039/c1gc15703e

Hu, L. F., Peng, H., Zhang, Y., Xia, Q., He, H. W., Ruan, R., Liu, Y. H., and Liu, A. H. (2020). "Insight into the interaction between arabinoxylan and imidazolium acetate-based ionic liquids," *Carbohydr. Polym.* 231, Article ID 115699. DOI: 10.1016/j.carbpol.2019.115699

Hunt, P. A., Ashworth, C. R., and Matthews, R. P. (2015). "Hydrogen bonding in ionic liquids," *Chem. Soc. Rev.* 44(5), 1257-1288. DOI: 10.1039/c4cs00278d

Klemm, D., Heublein, B., Fink, H. P., and Bohn, A. (2005). "Cellulose: Fascinating biopolymer and sustainable raw material," *Angew. Chem. Int. Ed.* 44(22), 3358-3393. DOI: 10.1002/anie.200460587

Krishna, G. M., and Jiang, J. W. (2015). "Cellulose dissolution and regeneration in ionic liquids: a computational perspective," *Chem. Eng. Sci.* 121, 180-189. DOI: 10.1016/j.ces.2014.07.025

Li, Y., Liu, X. M., Zhang, S. J., Yao, Y. Y., Yao, X. Q., Xu, J. L., and Lu, X. M. (2015).

"Dissolving process of a cellulose bunch in ionic liquids: A molecular dynamics study," *Phys. Chem. Chem. Phys*. 17(27), 17894-17905. DOI: 10.1039/c5cp02009c

Lungwitz, R., and Spange, S. (2008). "A hydrogen bond accepting (HBA) scale for anions, including room temperature ionic liquids," *New J. Chem.* 32(3), 392-394. DOI: 10.1039/b714629a

O'Sullivan, A. C. (1997). "Cellulose: The structure slowly unravels," *Cellulose* 4(3), 173-207. DOI: 10.1023/A:1018431705579

Pinkert, A., Marsh, K. N., Pang, S. S., and Staiger, M. P. (2009). "Ionic liquids and their interaction with cellulose," *Chem. Rev*. 109, 6712-6728. DOI: 10.1021/cr9001947

Sanchez-Badillo, J. A., Gallo, M., Rutiaga-Quinones, J. G., and Lopez-Albarran, P. (2021). "Solvent behavior of an ionic liquid set around a cellulose I*β* crystallite model through molecular dynamics simulations," *Cellulose* 28, 6767-6795. DOI: 10.1007/s10570-021-03992-7

Sanchez, P. B., Tsubaki, S., Padua, A. A. H., and Wada, Y. (2020). "Kinetic analysis of microwave-enhanced cellulose dissolution in ionic solvents," *Phys. Chem. Chem. Phys*. 22(3), 1103-1010. DOI: 10.1039/c9cp06239d

Sansaniwal, S. K., Rosen, M. A., and Tyagi, S. K. (2017). "Global challenges in the sustainable development of biomass gasification: An overview," *Renew. Sust. Energ. Rev*. 80, 23-43. DOI: 10.1016/j.rser.2017.05.215

Seddiqi, H., Oliaei, E., Honarkar, H., Jin, J. F., Geonzon, L. C., Bacabac, R. G., and Klein-Nulend, J. (2021). "Cellulose and its derivatives: Towards biomedical applications," *Cellulose* 28, 1893-1931. DOI: 10.1007/s10570-020-03674-w

Singh, S. K., and Savoy, A. W. (2020). "Ionic liquids synthesis and applications: An overview," *J. Mol. Liq*. 297, Article ID 112038. DOI: 10.1016/j.molliq.2019.112038

Usmani, Z., Sharma, M., Gupta, P., Karpichev, Y., Gathergood, N., Bhat, R., and Gupta, V. K. (2020). "Ionic liquid based pretreatment of lignocellulosic biomass for enhanced bioconversion," *Bioresource Technol.* 304, Article ID 123003. DOI: 10.1016/j.biortech.2020.123003

Valert, K. I. (2010). "Crystalline cellulose: Structure and hydrogen bonds," *Russ. Chem. Rev*. 79(3), 261-272. DOI: 10.1070/RC2010v079n03ABEH004065

Xia, Q., Peng, H., Yuan, L., Hu, L. F., Zhang, Y., and Ruan, R. (2020). "Anionic structural effect on the dissolution of arabinoxylan-rich hemicellulose in 1-butyl-3-methylimidazolium carboxylate-based ionic liquids," *RSC Adv.* 10, 11643-11651. DOI: 10.1039/c9ra10108j

Xiong, B., Zhao, P. P., Hu, K., Zhang, L. N., and Cheng, G. Z. (2014). "Dissolution of cellulose in aqueous NaOH/urea solution: Role of urea," *Cellulose* 21, 1183-1192. DOI: 10.1007/s10570-014-0221-7

Xu, A. R., Cao, L. L., Wang, B. J., and Ma, J. Y. (2015). "Dissolution behavior of cellulose in IL + DMSO solvent: Effect of alkyl length in imidazolium cation on cellulose dissolution," *Adv. Mater. Sci. Eng.* 2015(4), Article ID 406470. DOI: 10.1155/2015/406470

Xu, A. R., Wang, J. J., and Wang, H. Y. (2010). "Effects of anionic structure and lithium salts addition on the dissolution of cellulose in 1-butyl-3-methylimidazolium-based ionic liquid solvent system," *Green Chem.* 12(2), 268-275. DOI: 10.1039/b916882f

Xu, A. R., and Zhang, Y. B. (2015). "Insight into dissolution mechanism of cellulose in [C_4mim][CH_3COO]/DMSO solvent by ^{13}C NMR spectra," *J. Mol. Struct.* 1088, 101-104. DOI: 10.1016/j.molstruc.2015.02.031

Xu, A. R., Zhang, Y. B., Liu, W. W., Yao, K. S., and Xu, H. (2014). "Effect of alkyl

chain length in anion on dissolution of cellulose in 1-butyl-3-methylimidazolium carboxylate ionic liquids," *J. Mol. Liq.* 197, 211-214. DOI: 10.1016/j.molliq.2014.05.018

Zhang, J. M., Zhang, H., Wu, J., Zhang, J., He, J. S., and Xiang, J. F. (2010). "NMR spectroscopic studies of cellobiose solvation in EmimAc aimed to understand the dissolution mechanism of cellulose in ionic liquids," *Phys. Chem. Chem. Phys*. 12(8), 1941-1947. DOI: 10.1039/b920446f

Zhang, Y. H. R. (2008). "Reviving the carbohydrate economy *via* multi-product lignocellulose biorefineries," *J. Ind. Microbiol. Biotechnol.* 35(5), 367-375. DOI: 10.1007/s10295-007-0293-6

Zhao, Y. L., Liu, X. M., Wang, J. J., and Zhang, S. J. (2013). "Effects of anionic structure on the dissolution of cellulose in ionic liquids revealed by molecular simulation," *Carbohydr. Polym.* 94, 723-730. DOI: 10.1016/j.carbpol.2013.02.011

Article submitted: November 13, 2022; Peer review completed: December 3, 2022; Revised version received and accepted: January 5, 2023; Published: January 11, 2023.
DOI: 10.15376/biores.18.1.1590-1601